Conditional deletion of *Ccl2* in smooth muscle cells does not reduce early atherosclerosis in mice

Short title:

Conditional deletion of *Ccl2* in smooth muscle cells does not reduce early atherosclerosis in mice

Stine Gunnersen[1,2], Jeong Tangkjær Shim[1,2], Fan Liu[3], Uwe J.F. Tietge[3,4], Charlotte Brandt Sørensen[1,2], Jacob Fog Bentzon[1,2,5*]

[1]Department of Clinical Medicine, Aarhus University, Aarhus, Denmark

[2]Department of Cardiology, Aarhus University Hospital, Aarhus, Denmark

[3]Division of Clinical Chemistry, Department of Laboratory Medicine, Karolinska Institutet, Stockholm, Sweden

[4]Clinical Chemistry, Karolinska University Laboratory, Karolinska University Hospital, Stockholm, Sweden

[5]Centro Nacional de Investigaciones Cardiovasculares Carlos III (CNIC), Madrid, Spain

* jfbentzon@clin.au.dk

Abstract

Background: C-C motif chemokine ligand 2 (CCL2) is a pro-inflammatory chemokine important for monocyte recruitment to the arterial wall and atherosclerotic plaques. Global knockout of *Ccl2* reduces plaque formation and macrophage content in mice, but the importance of different plaque cell types in mediating this effect has not been resolved. Smooth muscle cells (SMCs) can adopt a potentially pro-inflammatory function with expression of CCL2. The present study aimed to test the hypothesis that SMC-secreted CCL2 is involved in early atherogenesis in mice.

Methods: SMC-restricted Cre recombinase was activated at 6 weeks of age in mice with homozygous floxed or wildtype *Ccl2* alleles. Separate experiments in mice lacking the Cre recombinase transgene were conducted to control for genetic background effects. Hypercholesterolemia and atherosclerosis were induced by a tail vein injection of recombinant adeno-associated virus (rAAV) encoding proprotein convertase subtilisin /kexin type 9 (PCSK9) and a high-fat diet for 12 weeks.

Results: Unexpectedly, mice with SMC-specific *Ccl2* deletion developed higher levels of plasma cholesterol and larger atherosclerotic plaques with more macrophages compared with wild-type littermates. When total cholesterol levels were incorporated into the statistical analysis, none of the effects on plaque development between groups remained significant. Importantly, changes in plasma cholesterol and atherosclerosis remained in mice lacking Cre recombinase indicating that they were not caused by SMC-specific CCL2 deletion but by effects of the floxed allele or passenger genes.

Conclusions: SMC-specific deficiency of *Ccl2* does not significantly affect plaque development in hypercholesterolemic mice.

45 **Introduction**

46 Atherosclerosis is a low-grade, non-resolving inflammatory disease driven by retention of
47 low-density lipoproteins (LDL) in the arterial wall [1]. Inhibition of inflammatory pathways
48 reduces plaque progression in experimental models and protects against the incidence of
49 clinical atherosclerotic events in patients with prior myocardial infarction [2,3]. Blocking
50 inflammation broadly in the body, however, adversely affects defenses against infection.
51 Research is needed to identify mechanisms that locally control inflammatory cells to devise
52 potent anti-inflammatory therapies that are specific or selective for atherosclerosis.

53 C-C motif chemokine ligand 2 (CCL2) is a pro-inflammatory chemokine secreted by multiple
54 cell types, which is central in the recruitment of monocytes to tissues and has a clear causal
55 role in atherosclerosis [4,5]. Global deficiency of *Ccl2* in *Apoe*$^{-/-}$ mice, *Ldlr*$^{-/-}$ mice, and mice
56 overexpressing apoB consistently inhibited atherogenesis and reduced plaque content of
57 macrophages [6–8]. Blocking *Ccl2* activity in mice with advanced atherosclerosis reduced
58 further plaque progression and changed plaque composition to contain fewer macrophages,
59 more SMCs, and more collagen [9]. These studies indicate a continued role of CCL2 that
60 extends beyond disease initiation. CCL2 is also expressed in human atherosclerotic plaques
61 and associated with features of plaque vulnerability,[10] and *CCL2* polymorphisms and
62 elevated CCL2 plasma levels are associated with an increased risk of cardiovascular
63 disease [10–12].

64 Expression in myeloid cells accounts for a part of the atherosclerosis-promoting effect of
65 CCL2 in mice [13], but local arterial cells also express CCL2 and may carry some of the
66 proatherogenic effect [4,14,15]. Several studies have suggested roles for modulated SMCs
67 in controlling plaque inflammation. Cultured SMCs can be induced by interleukin-1β (IL-1β)
68 and minimal modified low-density lipoprotein particles (mmLDL) to express CCL2 and other

69 pro-inflammatory genes [16,17]. In *Ldlr*$^{-/-}$ mice, SMC-specific deficiency of inhibitor of
70 nuclear factor kappa B kinase subunit beta (IKKβ), a catalytic subunit necessary for
71 activation of nuclear factor kappa B (NF-κB) that is upstream of *Ccl2* expression, had
72 multiple metabolic effects, including adipose tissue changes and reduced plaque
73 development [18]. Furthermore, SMC-specific conditional knockout of the interleukin-1
74 receptor (IL-1R) substantially reduced plaque formation in *Apoe*$^{-/-}$ mice [19]. Recently, a
75 lineage-tracing study in mice suggested dichotomous roles of SMC-derived CCL2 in
76 atherosclerosis development depending on the phenotypical modulation state of the SMCs
77 [20]. These studies indicate the presence of important effector functions of modulated SMCs
78 for controlling plaque inflammation and progression, but the nature of these is only sparsely
79 understood. In the present study, we assessed the importance of SMC-secreted CCL2 for
80 early atherosclerosis in hypercholesterolemic mice.
81
82

Materials and methods

Please see an expanded methods section in the S1 Supporting information.

Mice

Male *Myh11*-CreER^{T2} mice (B6.FVB-Tg(Myh11-cre/ERT2)1Soff/J, stock no. 019079) expressing tamoxifen-inducible Cre recombinase (*CRE-ERT2)* under the SMC-specific myosin heavy chain 11 (*Myh11*) promotor [21], and *Ccl2*$^{flx/flx}$ mice (B6N.129S1(FVB)-Ccl2tm1.2Tyos/J, stock no. 023347) with *loxP* sites flanking exon 1-2 of the *Ccl2* gene [22] were acquired from Jackson and intercrossed. Experimental mice of our study were male offspring of breeders heterozygous for the floxed *Ccl2* allele. Only males were included because the Myh11-CreER^{T2} transgene is inserted on the Y chromosome. One of the male breeders was found without the Y-linked *Myh11-CreER^{T2}*, presumably due to the exchange in genetic material between pseudoautosomal regions of X and Y chromosomes [23,24], and was used to breed CreER^{T2}-negative male mice for control experiments. Animals were housed in groups with unlimited access to tap water and a standard laboratory diet in an enriched environment with standard bedding and nesting material under a 12/12 h day-night cycle in a temperature (20-25ºC) controlled facility.

At 6-8 weeks of age, male *Myh11*-CreER^{T2} x *Ccl2*$^{flx/flx}$ and *Myh11*-CreER^{T2} x *Ccl2*$^{wt/wt}$ littermates were injected i.p. with 1 mg tamoxifen (T5648, Sigma-Aldrich) dissolved in corn oil (P2144, Sigma-Aldrich) daily for 10 days to obtain mice with or without SMC-specific *Ccl2* deletion (*Ccl2*$^{SMC-KO}$ and *Ccl2*$^{SMC-WT}$). Male *Ccl2*$^{flx/flx}$ and *Ccl2*$^{wt/wt}$ littermates were treated similarly. At 12 weeks of age, hypercholesterolemia was induced by a single tail vein injection of rAAV8-D377Y-mPCSK9 virus particles (rAAV-PCSK9, 1×10^{11} vector genomes,

107 produced at Vector Core at the University of North Carolina, Chapel Hill, North Carolina,
108 USA) and shifted to a high-fat diet (D12079B, Research Diets Inc.) containing 21% fat and
109 0.2% cholesterol [25]. After 12 weeks of feeding atherosclerosis-promoting diet, the mice
110 were anesthetized with 5 mg pentobarbital and 4 mg lidocain i.p. and terminated by
111 exsanguination. The arterial tree was perfused with Cardioplex for 30 seconds and 4%
112 phosphate-buffered formaldehyde (PFA) for 5 minutes at 100 mmHg through the left
113 ventricle, followed by immersion-fixation in 4% PFA for 24 hours. Animal procedures were
114 approved by The Danish Animal Experiments Inspectorate (license 2015-15-0201-00542)
115 and conducted at Aarhus University following ARRIVE guidelines.
116

117 **Atherosclerosis analysis**

118 The top half of the heart containing the aortic root was removed and embedded in paraffin.
119 Transversal sections (3 μm) of the aortic root were cut from the distal part of the heart and
120 serial sections were collected at 0 μm, 80 μm, 160 μm and 240 μm from the level of the
121 aortic valve commissures. For quantification of atherosclerosis, sections from all levels
122 (main experiment) or the first two levels (control experiment with Cre-negative mice) were
123 stained by orcein. Sections from the first level (main experiment) were stained for smooth
124 muscle alpha-2 actin (ACTA2) and galectin 3 (LGALS3) using mouse monoclonal anti-
125 ACTA2 (Dako, cat. no. M0851, 1:100) after blocking with Fab fragment (Jackson
126 ImmunoResearch, cat. no. 715-007-003, 1:10) and rat monoclonal IgG2a anti-LGALS3
127 (Cederlane, cat. no. CL8942AP, 1:250) followed by Alexa 488-conjugated donkey anti-
128 mouse (Invitrogen, cat. no. A21202, 1:400) or Alexa 488-conjugated donkey anti-rat
129 (Invitrogen, cat. no. A21208, 1:400) secondary antibodies. Analysis of stained sections was
130 performed in Fiji (also known as ImageJ) [26].

131 Aortae were cleaned of all periadventitial fat, cut open longitudinally, stained with Oil Red O
132 for 10 minutes at 37˚C, washed in isopropanol and PBS, and mounted on a microscope slide
133 with Aquatex for en face quantification of lesion coverage in the aortic arch down to the
134 supreme intercostal artery. Analysis of the scanned slides was performed in Fiji.
135

136 **Human atherosclerotic plaques**

137 Human atherosclerotic plaques from the left anterior descending artery obtained from a
138 previously published material [23] were used for immunohistochemical analysis of CCL2
139 localization using rabbit polyclonal anti-CCL2 (Lifespan Bioscience, cat. no. LS-B10540,
140 1:50) and Envision+ System-HRP (DAB) (Dako, cat. no. K4010). The original material was
141 collected after approval by the regional ethical committee [23]. It was subsequently
142 anonymized and did not require further ethical approval for the use in the present study.
143

144 **Cell studies**

145 An immortalized murine smooth muscle cell line (MOVAS, ATCC CRL-2797) was
146 maintained in culture in DMEM (Fischer Scientific, cat. no. 41965062) supplemented with
147 10% fetal calf serum (FCS) (Sigma-Aldrich, cat. no. F7524), 1% penicillin-streptomycin
148 (Invitrogen, cat. no. 15140122) and 1% gentamycin (G418, Invivogen cat. no. ant-gn-1).
149 Primary human aortic SMCs (hVSMCs), obtained as previously described [24], were kindly
150 provided by Thomas Ledet, Aarhus University. They were maintained in DMEM
151 supplemented with 10% FCS and 1% penicillin-streptomycin. Incubation was performed at
152 37˚C in a humidified atmosphere of 95% air and 5% CO_2 and the medium was changed
153 every 2-3 days. MOVAS cells were seeded for experiments in 12-well plates at a density of
154 6.25×10^3 cells/cm^2, and human SMCs were seeded in 6-well plates with a density of 1.6×10^4

155 cells/cm^2. The experiments were performed 24 h after seeding the cells. To induce an
156 inflammatory response in hVSMCs and MOVAS cells, the cells were incubated with IL-1β
157 (R&D Diagnostics, cat. no. 401-ML-005/CF, 0.01 – 100 ng/ul) for 24 hours. The conditioned
158 media (CM) were then collected and cleared from debris by centrifugation (3,000xg for 5
159 min). CCL2 levels were measured in conditioned media by ELISA (Invitrogen, cat nos. 88-
160 7391-88 and 88-7399-88).
161
162 **Statistics**
163 All statistical analysis was performed using GraphPad Prism 9 (GraphPad Software Inc.).
164 Data was checked for normal and log-nomal distribution and equal variance and analyzed
165 using the tests indicated in figure legends. Multiple regression analysis was used to analyze
166 associations with plaque data using genotype and plasma cholesterol as independent
167 variables and associations with plasma cholesterol levels (using genotype and plasma
168 PCSK9 concentrations as independent variables). *P* values below 0.05 were defined as
169 statistically significant. Data are shown as mean ± standard error of the mean (SEM) as
170 indicated in each figure legend. The number of animals/samples analyzed is stated in figure
171 legends. In some analyses, data points were not obtained for all mice because of technical
172 failures. All procedures and analyses were performed blinded for the mouse genotype.
173
174
175

176 **Results**

177

178 **CCL2 is expressed in human atherosclerotic lesions**

179 To evaluate the expression pattern of CCL2 during human atherogenesis, we performed
180 CCL2 immunohistochemistry in human coronary lesions of different severity (Fig 1A). CCL2
181 was found expressed in normal human coronary artery in both the medial and intimal layer.
182 In early lesions, CCL2 was present in foam cells, but also in the underlying artery wall. In
183 advanced atherosclerotic lesions, CCL2 was detected in areas adjacent to the necrotic core,
184 while CCL2 expression in the medial layer was diminished. Staining of adjacent sections
185 with ACTA2 showed considerable overlap with the pattern of CCL2 staining suggesting
186 widespread SMC expression of CCL2 in normal media/intima as well as in developing
187 plaques.

188 **Fig 1. CCL2 expression in SMC-rich regions of human plaques and CCL2 secretion in**
189 **SMC cultures.** (A) CCL2 (brown color) and ACTA2 (red color) detected by
190 immunohistochemistry in adjacent sections of normal human artery wall and atherosclerotic
191 lesions of different severity. CCL2 is expressed in media and intima of the normal arterial
192 wall. CCL2 is also expressed in foam cells and underlying medial SMCs, and in active
193 inflammatory areas adjacent to the necrotic core in the fibroatheroma. F, foam cells. I,
194 Intima. M, Media, NC, necrotic core. Scale bars = 100 μm. CCL2 is secreted from cultured
195 SMCs stimulated with IL-1β. CCL2 levels measured in conditioned media (CM) from (B)
196 MOVAS cells (n=6 replicates per group) and (C) hVSMCs (n=5-6 replicates per group)
197 treated with IL-1β for 24 hours. (D) Flow cytometry measurement of intracellular CCL2
198 accumulation in MOVAS cells after blocking the secretory pathway by Brefeldin-A. IL-1β
199 stimulation (1 ng/ml) increases CCL2 accumulation measured as median fluorescent

200 intensity (n=3 replicates per group). Graphs show mean ± SEM. *p<0.05, **p<0.01,
201 ***p<0.001, ****p<0.0001 by Dunnett´s T3 multiple comparisons test following Brown-
202 Forsythe ANOVA (A,B) and unpaired Student´s t-test (D).
203
204 **Human and murine SMCs in culture can be stimulated to express CCL2**
205 Previous studies have reported CCL2 secretion from murine SMCs upon stimulation [27].
206 To confirm this, we stimulated human VSMCs and a murine SMC line (MOVAS) with IL-1β
207 and found that the secretion of CCL2 in the conditioned media of both increased dose-
208 dependently (Fig 1B-C). Also, assessed by flow cytometry, we found an increase in protein
209 expression of CCL2 in response to IL-1β stimulation of MOVAS cells (Fig 1D).
210
211 **SMC-specific conditional knockout of *Ccl2* in hypercholesterolemic mice**
212 Modulation to a CCL2-secreting SMC phenotype by local IL-1β or other pro-inflammatory
213 stimuli could facilitate ongoing inflammation in the developing atherosclerotic lesion. To test
214 this hypothesis *in vivo*, we crossed mice with SMC-restricted CreER^{T2} expression and either
215 homozygous floxed or wildtype *Ccl2* alleles to obtain mice with SMC-specific deletion of
216 *Ccl2* (*Ccl2*$^{SMC-KO}$) and littermate controls (*Ccl2*$^{SMC-WT}$) (Fig 2A). Mean allelic recombination
217 efficiency was 75.9 ± 1.3% (mean ± SEM) (Fig 2B). Because recombination was determined
218 in aortic samples after mechanical removal of the adventitia and endothelium, the analyzed
219 cells may have contained a small amount of non-SMC cell types causing some
220 underestimation of recombination efficiency.
221 **Fig 2. Experimental design.** (A) Illustration of the genetic alterations in *Myh11*-CreER^{T2} x
222 *Ccl2*$^{flx/flx}$ mice that lead to SMC-specific knockout of *Ccl2* after tamoxifen injection. Black
223 arrows flanking the left loxP site indicate primers used for detecting recombination by qPCR.

224 (B) Recombination efficiency was measured as the reduction in (non-recombined) floxed
225 CCL2 alleles in genomic DNA of the aortic media in *Myh11*-CreER^{T2} x *Ccl2*$^{flx/flx}$ (n=21, grey
226 bar) compared with *Ccl2*$^{flx/flx}$ (n=15, black bar) mice. The graph shows mean ± SEM.
227 ****p<0.0001 by unpaired Welch t-test. (C) Schematic illustration of the mouse experiment
228 showing the timing of tamoxifen injections (10 daily doses between 6-8 weeks of age),
229 induction of LDL receptor-deficiency by a single tail-vein injection of rAAV8-D377Y-mPCSK9
230 at 12 weeks of age, and final analysis after feeding Western-type diet for 12 weeks. Blood
231 samples were collected 2, 6, and 11 weeks after rAAV-PCSK9 injection.
232
233 **Increased plasma cholesterol levels in *Ccl2*$^{SMC-KO}$ mice**
234 Atherosclerosis was induced in *Ccl2*$^{SMC-KO}$ and *Ccl2*$^{SMC-WT}$ mice by rAAV-PCSK9 injection
235 followed by feeding a high-fat diet for 12 weeks (Fig 2C). Plasma cholesterol was similar in
236 the two genotypes after 2 weeks but significantly higher in *Ccl2*$^{SMC-KO}$ mice than *Ccl2*$^{SMC-WT}$
237 mice at both 6 and 11 weeks (Fig 3A). Analysis of size-fractioned lipoproteins measured at
238 12 weeks showed that the increased cholesterol in *Ccl2*$^{SMC-KO}$ mice was in apoB-containing
239 lipoproteins (VLDL and LDL) (Fig 3B).
240 **Fig 3. Plasma cholesterol phenotype.** (A) Plasma cholesterol levels were initially similar
241 but significantly increased in *Ccl2*$^{SMC-KO}$ (n=22, orange circles) compared with *Ccl2*$^{SMC-WT}$
242 (n=24, blue squares) mice at 6 and 11 weeks after rAAV-PCSK9 injection. (B) Analysis of
243 size-fractionated lipoproteins by FPLC at 12 weeks after rAAV-PCSK9 injection revealed
244 increases in cholesterol in VLDL- and LDL-sized, but not HDL-sized, lipoproteins. (C) Sterol
245 analysis for markers of cholesterol biosynthesis (lathosterol and desmosterol) or cholesterol
246 absorption (campesterol, stigmasterol, sitosterol, lanosterol) showed no significant changes
247 or changes opposite the direction that could explain the increased plasma cholesterol levels

248 in *Ccl2*$^{SMC-KO}$ (n=23) compared with *Ccl2*$^{SMC-WT}$ mice (n=21). Plasma PCSK9 levels were not
249 different between *Ccl2*$^{SMC-WT}$ (n=22) and *Ccl2*$^{SMC-KO}$ mice (n=24) (D). (E) Plasma cholesterol
250 levels were numerical increased, though not statistically significant, in *Cre*-negative *Ccl2*$^{flx/flx}$
251 (n=15, black squares) compared with *Ccl2*$^{wt/wt}$ (n=17, grey triangles) mice 11 weeks after
252 rAAV-PCSK9 injection. Graphs show mean ± SEM. *p<0.05; **p<0.01; NS, not statistically
253 significant in a mixed-effects model for repeated measurements with Šidák´s multiple
254 comparison test (A,D,E) and Welch t-test (C).
255 Sterol analysis was performed to provide clues to the source of the increased plasma
256 cholesterol in *Ccl2*$^{SMC-KO}$ mice (Fig 3C)[28]. Markers for the rate of cholesterol synthesis
257 (lathosterol and desmosterol) and intestinal cholesterol absorption (campesterol,
258 stigmasterol, sitosterol, lanosterol) were either unchanged or reduced in plasma of *Ccl2*$^{SMC-}$
259 ^{KO} compared with *Ccl2*$^{SMC-WT}$ mice. These observations instead pointed towards a potential
260 difference in LDL clearance, which could be caused by a difference in rAAV8 transduction
261 efficiencies leading to differences in PCSK9 levels. We therefore measured plasma PCSK9
262 levels in samples taken at 2 and 11 weeks after rAAV8. Plasma PCSK9 levels increased
263 from 2 to 11 weeks, but no statistically significant differences were found between *Ccl2*$^{SMC-}$
264 ^{KO} and *Ccl2*$^{SMC-WT}$ mice (Fig 3D). Furthermore, introducing plasma PCSK9 levels in multiple
265 regression analysis did not weaken the link between genotype and plasma cholesterol levels
266 (S2 Table).
267 Although the floxed *Ccl2* mice were already backcrossed into the B6 mouse background 10
268 times when we acquired them and further 3-4 times in our facility, a region around the *Ccl2*
269 locus will be derived from the 129S1 embryonic stem cells in which the *Ccl2* gene targeting
270 was performed [26]. This passenger gene region could potentially harbor plasma cholesterol
271 regulating loci. Furthermore, the genetic modification of the *Ccl2* locus could affect

272 neighboring gene expression in any cell type, which in theory could impact lipoprotein
273 metabolism. To explore this, we also analyzed plasma lipids in CreER^{T2}-negative *Ccl2*$^{flx/flx}$
274 and *Ccl2*$^{wt/wt}$ mice that had been subjected to a similar regimen of rAAV8-PCSK9 treatment
275 and high-fat diet. We found a numerical increase in plasma cholesterol levels in *Ccl2*$^{flx/flx}$
276 compared with *Ccl2*$^{wt/wt}$ at the last time point (Fig 3E). Although this difference was not
277 significant (p=0.08*)*, it is consistent with genetic background effects, rather than the SMC-
278 specific *Ccl2* deletion, being the underlying cause of the differences in plasma cholesterol.
279

280 **Atherosclerosis development**

281 Atherosclerosis development was assessed in sections of the aortic root and by en face
282 analysis of the aortic arch after 12 weeks of hypercholesterolemia (Fig 4A-B). Aortic root
283 plaque area was significantly increased in *Ccl2*$^{SMC-KO}$ compared with *Ccl2*$^{SMC-WT}$ mice (Fig
284 4C). In the aortic arch, the lesion coverage showed an insignificant tendency towards an
285 increase in *Ccl2*$^{SMC-KO}$ compared with wildtype littermates (Fig 4D).

286 **Fig 4**. **Quantification of atherosclerosis after 12 weeks of atherogenic diet feeding**.
287 Representative images of (A) hematoxylin-eosin-stained cross sections from the aortic root,
288 and (B) Oil Red O-stained aortic arches opened for en face quantification. Scale bars = 400
289 μm (A) and 2 mm (B). (C) Plaque size was statistically significantly increased in *Ccl2*$^{SMC-KO}$
290 (n=14, orange circles) mice compared with *Ccl2*$^{SMC-WT}$ (n=14, blue squares) mice in the
291 aortic root. (D) In the aortic arch, a similar tendency was seen but not statistically significant
292 (*Ccl2*$^{SMC-KO}$, n=24; *Ccl2*$^{SMC-WT}$, n=21). Aortic root plaque size was also statistically
293 significantly increased in *Cre*-negative *Ccl2*$^{flx/flx}$ (black squares, n=12) mice compared with
294 *Ccl2*$^{wt/wt}$ (grey triangles, n=10) (E). Graphs show mean ± SEM. * p<0.05, NS, not statistically
295 significant by Welch t-test on log-transformed data.

296 Aortic root cross-sections were analyzed for plaque cellular composition using the
297 macrophage marker LGALS3 and the SMC-marker ACTA2 (Fig 5A). LGALS3 can be
298 expressed on SMC lineage cells in addition to macrophages. Still, we have previously found
299 that the level of misclassification by standard immune fluorescent staining in PCSK9-
300 induced atherosclerosis is minor as assessed by SMC lineage tracing [29]. The number of
301 LGALS3+ cells was increased in *Ccl2*$^{SMC-KO}$ compared with wildtype littermates (Fig 5B),
302 while the number of ACTA2+ cells was unaffected (Fig 5C).

303 **Fig 5. Plaque composition in the aortic root after 12 weeks of atherosclerosis**
304 **development.** (A) Representative images showing LGALS3+ cells (green), ACTA2+ cells
305 (red), and merged channels with DAPI (blue) from *Ccl2*$^{SMC-WT}$ and *Ccl2*$^{SMC-KO}$ mice. Scale
306 bars 200 μm. Number of plaque LGALS3+ cells (*Ccl2*$^{SMC-WT}$, n=14; *Ccl2*$^{SMC-KO}$, n=15) (B),
307 number of ACTA2+ cells (*Ccl2*$^{SMC-WT}$, n=15; *Ccl2*$^{SMC-KO}$, n=16) (D) and number of
308 ACTA2/LGALS3 double-negative cells (*Ccl2*$^{SMC-WT}$, n=16; *Ccl2*$^{SMC-KO}$, n=14) in aortic root
309 sections from *Ccl2*$^{SMC-WT}$ (blue squares) and *Ccl2*$^{SMC-KO}$ (orange circles). Graphs show
310 mean ± SEM. *p<0.05; NS, not statistically significant by Welch t-test on log-transformed
311 data.

312 Murine atherosclerotic lesions also contain a large population of SMC lineage cells that lose
313 expression of ACTA2 and modulate to other forms [30]. We therefore also quantified
314 ACTA2/LGALS3 double-negative cells (ACTA2-/LGALS3-), which are enriched for
315 modulated plaque SMCs, but found no differences between the two groups (Fig 5D).

316 None of the differences in atherosclerosis measures between groups were statistically
317 significant in a multiple regression model incorporating final plasma cholesterol (data not
318 shown) or the area-under-the-curve of plasma cholesterol levels from 2 until 11 weeks (S3
319 and S4 Tables). This indicates that the observed changes were explained by the unexpected

320 differences in plasma cholesterol between groups, which was unrelated to the deletion of
321 Ccl2 in SMCs. This was confirmed by analysis of aortic root plaque area in CreER^{T2}-negative
322 *Ccl2*$^{flx/flx}$ and *Ccl2*$^{wt/wt}$ mice (Fig 4E). As observed for the *Ccl2*$^{SMC-KO}$ mice, the plaque area
323 was significantly increased in *Ccl2*$^{flx/flx}$ mice compared to their wildtype counterparts,
324 supporting the conclusion that secretion of CCL2 by modulated SMCs in the plaque is not
325 an important mediator in plaque development.
326
327
328

329 **Discussion**

330 SMCs have traditionally been considered to have a protective role in atherosclerosis by
331 producing fibrous tissue that stabilizes the plaque and protects it from rupture and thrombotic
332 complications [31]. Over the last decade, however, multiple studies have revisited the role
333 of SMCs in atherosclerosis using mouse models and lineage-tracing techniques [30]. Such
334 experiments have shown that plaque SMCs derive from a small group of arterial SMCs that
335 undergo clonal expansion and modulate to cells with fibroblast-like (aka. fibromyocytes) and
336 chondrocyte-like (aka. chondromyocytes) phenotypes [32–37]. Some of these show
337 evidence of inflammatory signaling,[38] but the causal role of this for plaque development is
338 still sparsely understood.

339 In the present study, we tested whether the ability of SMCs to secrete the proinflammatory
340 cytokine CCL2 is a mediator linking SMC modulation to arterial inflammation and plaque
341 development. CCL2 is a central cytokine involved in monocyte recruitment to tissues, and
342 global knockout of *Ccl2* reduces plaque formation and progression in mice [6–8,13]. We
343 confirmed the expression of CCL2 in human plaques in SMC-rich areas including the arterial
344 media in the pre-diseased arterial wall. Furthermore, we confirmed the ability of both human
345 and mouse SMCs to respond to an inflammatory stimulus with CCL2 expression. To test the
346 potential causal role of this, we studied atherosclerosis in mice with SMC-specific conditional
347 knockout of *Ccl2*. Unexpectedly, we found increased hypercholesterolemia and
348 atherosclerosis in mice with SMC-specific deficiency of *Ccl2* compared with wildtypes
349 littermates.

350 A recent study by Owsiany et al. also found increased atherosclerosis and macrophage
351 recruitment in *Apoe*$^{-/-}$ mice with heterozygous, but not homozygous, knockout of *Ccl2* in
352 SMCs [20]. The increased atherosclerosis in heterozygous animals appeared to result from

353 increased monocytosis in combination with a preserved ability to recruit monocytes into the
354 arterial intima, which was lost in homozygous animals [20]. Recombination rates were not
355 quantified in the study of Owsiany et al. and hence it is difficult to compare our mice (with
356 an app. 75% recombination rate of the floxed *Ccl2* locus) with the two genotypes reported
357 in that study. Notably, even though our findings may on the surface seem consistent with
358 the increased atherosclerosis reported in the heterozygous mice in Owsiany et al., the
359 proatherogenic effect in our experiments was not caused by *Ccl2* deletion since it also
360 occurred in the absence of Cre activity. Rather it was explained by genetic differences
361 between the floxed and wildtype *Ccl2* allele; either the floxing of the gene itself or passenger
362 gene variants in linkage disequilibrium with the *Ccl2* locus originating from the 129S1
363 embryonic stem cells used to create the mouse line [22,39]. One cannot conclude, however,
364 that such effects influenced the results of Owsiany et al. that used a different floxed *Ccl2*
365 mouse line, which was created using C57BL/6J embryonic stem cells [20,40]. Overall, we
366 conclude that the knockout of *Ccl2* in SMCs in our experimental context did not change
367 atherogenesis, similar to the homozygous SMC knockout in Owsiany et al. [20].
368 It should be noted that upregulation of both *Ccl7* (*Mcp3)* and *Ccl12* (*Mcp5)* located
369 downstream of the *Ccl2* gene was originally demonstrated for the mouse line used in our
370 studies upon Cre-mediated deletion of the floxed *Ccl2*-region [22]. Given that both encoded
371 proteins are also ligands for the C-C chemokine receptor type 2 (CCR2), potential
372 compensating effects from these genes cannot be excluded.
373 The genetic background effect appeared to accelerate atherosclerosis at least partly by
374 increasing hypercholesterolemia. Plasma cholesterol was significantly increased in *Ccl2*$^{SMC-}$
375 ^{KO} compared with *Ccl2*$^{SMC-WT}$ mice, which was unexpected since previous studies of mice
376 with global CCL2 knockout or overexpression did not show any effects on plasma

377 cholesterol levels [6–8,13]. Although the differences in plasma cholesterol levels in *Ccl2*$^{flx/flx}$
378 and *Ccl2*$^{wt/wt}$ mice (without the *Cre* transgene) were not statistically significant, they
379 resembled those of the main study indicating a genetic background effect. The differences
380 were not caused by differences in the efficiency of rAAV-PCSK9 transduction since the
381 effect was not present after 2 weeks but developed over time and plasma PCSK9 levels
382 were similar between groups in the two genotypes. The most likely explanation for the
383 differences in hypercholesterolemia may therefore be passenger gene variants in linkage
384 disequilibrium with the *Ccl2* locus.
385
386 *Strengths and limitations*
387 Our study has limitations. Recombination of CCL2 alleles in SMCs was not complete as is
388 generally the case in conditional knockout studies. This raises the question whether more
389 robust inhibition of CCL2 secretion from SMCs would have had an effect on plaque
390 development. It is also possible that remaining CCL2-competent SMCs could outcompete
391 recombined cells during clonal expansion in plaques if CCL2 secretion confers a survival
392 benefit. Finally, our studies were not designed to investigate the impact of SMC-specific
393 knockout on monocyte trafficking, which would have been relevant on the background of the
394 recent findings by Owsiany et al. [20].
395
396 **Conclusions**
397 Conditional deletion of *Ccl2* in SMCs does not inhibit the development of atherosclerosis in
398 mice with PCSK9-induced hypercholesterolemia.
399
400

401 **Supporting information**

402 **S1 Supporting information. Supplemental methods and references.**

403 **S2 Table. Determinants of plasma total cholesterol.**

404 **S3 Table. Determinants of plaque area in *Ccl2*$^{SMC-KO}$ and *Ccl2*$^{SMC-WT}$ mice.**

405 **S4 Table. Determinants of plaque LGALS3+ cells in *Ccl2*$^{SMC-KO}$ and *Ccl2*$^{SMC-WT}$ mice.**

406

407 **Acknowledgments**

408 We thank Lisa Maria Røge and Dorte Qualmann for excellent technical assistance.

409

410 **Author contributions**

411 **Conceptualization:** Stine Gunnersen, Jacob F. Bentzon

412 **Investigation:** Stine Gunnersen, Fan Liu, Uwe J.F. Tietge, Jeong T. Shim

413 **Methodology:** Stine Gunnersen, Charlotte B. Sørensen

414 **Supervision:** Charlotte B. Sørensen, Jacob F. Bentzon

415 **Writing – original draft:** Stine Gunnersen, Charlotte B. Sørensen, Jacob F. Bentzon

416 **Writing – review & editing:** Stine Gunnersen, Fan Liu, Uwe J.F. Tietge, Jeong T. Shim,

417 Charlotte B. Sørensen, Jacob F. Bentzon

418 **References**

419 1. Soehnlein O, Libby P. Targeting inflammation in atherosclerosis - from experimental
420 insights to the clinic. Nat Rev Drug Discov. 2021;20: 589–610. doi:10.1038/s41573-
421 021-00198-1

422 2. Ridker PM, Everett BM, Thuren T, MacFadyen JG, Chang WH, Ballantyne C, et al.
423 Antiinflammatory Therapy with Canakinumab for Atherosclerotic Disease. N Engl J
424 Med. 2017;377: 1119–1131. doi:10.1056/NEJMoa1707914

425 3. Tardif J-C, Kouz S, Waters DD, Bertrand OF, Diaz R, Maggioni AP, et al. Efficacy and
426 Safety of Low-Dose Colchicine after Myocardial Infarction. N Engl J Med. 2019;381:
427 2497–2505. doi:10.1056/NEJMoa1912388

428 4. Deshmane SL, Kremlev S, Amini S, Sawaya BE. Monocyte chemoattractant protein-1
429 (MCP-1): an overview. J Interferon Cytokine Res. 2009;29: 313–326.
430 doi:10.1089/jir.2008.0027

431 5. Yadav A, Saini V, Arora S. MCP-1: chemoattractant with a role beyond immunity: a
432 review. Clin Chim Acta. 2010;411: 1570–1579. doi:10.1016/j.cca.2010.07.006

433 6. Combadière C, Potteaux S, Rodero M, Simon T, Pezard A, Esposito B, et al.
434 Combined inhibition of CCL2, CX3CR1, and CCR5 abrogates Ly6C(hi) and Ly6C(lo)
435 monocytosis and almost abolishes atherosclerosis in hypercholesterolemic mice.
436 Circulation. 2008;117: 1649–1657. doi:10.1161/CIRCULATIONAHA.107.745091

437 7. Gu L, Okada Y, Clinton SK, Gerard C, Sukhova GK, Libby P, et al. Absence of
438 monocyte chemoattractant protein-1 reduces atherosclerosis in low density lipoprotein
439 receptor-deficient mice. Mol Cell. 1998;2: 275–281. doi:10.1016/s1097-
440 2765(00)80139-2

441 8. Gosling J, Slaymaker S, Gu L, Tseng S, Zlot CH, Young SG, et al. MCP-1 deficiency
442 reduces susceptibility to atherosclerosis in mice that overexpress human
443 apolipoprotein B. J Clin Invest. 1999;103: 773–778. doi:10.1172/JCI5624

444 9. Inoue S, Egashira K, Ni W, Kitamoto S, Usui M, Otani K, et al. Anti-Monocyte
445 Chemoattractant Protein-1 Gene Therapy Limits Progression and Destabilization of
446 Established Atherosclerosis in Apolipoprotein E–Knockout Mice. Circulation.
447 2002;106: 2700–2706. doi:10.1161/01.CIR.0000038140.80105.AD

448 10. Georgakis MK, van der Laan SW, Asare Y, Mekke JM, Haitjema S, Schoneveld AH,
449 et al. Monocyte-Chemoattractant Protein-1 Levels in Human Atherosclerotic Lesions
450 Associate With Plaque Vulnerability. Arterioscler Thromb Vasc Biol. 2021;41: 2038–
451 2048. doi:10.1161/ATVBAHA.121.316091

452 11. McDermott DH, Yang Q, Kathiresan S, Cupples LA, Massaro JM, Keaney JF, et al.
453 *CCL2* Polymorphisms Are Associated With Serum Monocyte Chemoattractant
454 Protein-1 Levels and Myocardial Infarction in the Framingham Heart Study.
455 Circulation. 2005;112: 1113–1120. doi:10.1161/CIRCULATIONAHA.105.543579

456 12. Nelken NA, Coughlin SR, Gordon D, Wilcox JN. Monocyte chemoattractant protein-1
457 in human atheromatous plaques. J Clin Invest. 1991;88: 1121–1127.
458 doi:10.1172/JCI115411

459 13. Aiello RJ, Bourassa PA, Lindsey S, Weng W, Natoli E, Rollins BJ, et al. Monocyte
460 chemoattractant protein-1 accelerates atherosclerosis in apolipoprotein E-deficient
461 mice. Arterioscler Thromb Vasc Biol. 1999;19: 1518–1525.
462 doi:10.1161/01.atv.19.6.1518

463 14. Schober A, Zernecke A, Liehn EA, von Hundelshausen P, Knarren S, Kuziel WA, et
464 al. Crucial role of the CCL2/CCR2 axis in neointimal hyperplasia after arterial injury in
465 hyperlipidemic mice involves early monocyte recruitment and CCL2 presentation on
466 platelets. Circ Res. 2004;95: 1125–1133. doi:10.1161/01.RES.0000149518.86865.3e

467 15. Yu X, Dluz S, Graves DT, Zhang L, Antoniades HN, Hollander W, et al. Elevated
468 expression of monocyte chemoattractant protein 1 by vascular smooth muscle cells in
469 hypercholesterolemic primates. Proc Natl Acad Sci USA. 1992;89: 6953–6957.
470 doi:10.1073/pnas.89.15.6953

471 16. Alexander MR, Murgai M, Moehle CW, Owens GK. Interleukin-1β modulates smooth
472 muscle cell phenotype to a distinct inflammatory state relative to PDGF-DD via NF-
473 κB-dependent mechanisms. Physiol Genomics. 2012;44: 417–429.
474 doi:10.1152/physiolgenomics.00160.2011

475 17. Cushing SD, Berliner JA, Valente AJ, Territo MC, Navab M, Parhami F, et al.
476 Minimally modified low density lipoprotein induces monocyte chemotactic protein 1 in
477 human endothelial cells and smooth muscle cells. Proc Natl Acad Sci USA. 1990;87:
478 5134–5138. doi:10.1073/pnas.87.13.5134

479 18. Sui Y, Park S-H, Xu J, Monette S, Helsley RN, Han S-S, et al. IKKβ links vascular
480 inflammation to obesity and atherosclerosis. J Exp Med. 2014;211: 869–886.
481 doi:10.1084/jem.20131281

482 19. Gomez D, Baylis RA, Durgin BG, Newman AAC, Alencar GF, Mahan S, et al.
483 Interleukin-1β has atheroprotective effects in advanced atherosclerotic lesions of
484 mice. Nat Med. 2018;24: 1418–1429. doi:10.1038/s41591-018-0124-5

485 20. Owsiany KM, Deaton RA, Soohoo KG, Tram Nguyen A, Owens GK. Dichotomous
486 Roles of Smooth Muscle Cell-Derived MCP1 (Monocyte Chemoattractant Protein 1) in
487 Development of Atherosclerosis. Arterioscler Thromb Vasc Biol. 2022;42: 942–956.
488 doi:10.1161/ATVBAHA.122.317882

489 21. Wirth A, Benyó Z, Lukasova M, Leutgeb B, Wettschureck N, Gorbey S, et al. G12-
490 G13-LARG-mediated signaling in vascular smooth muscle is required for salt-induced
491 hypertension. Nat Med. 2008;14: 64–68. doi:10.1038/nm1666

492 22. Takahashi M, Galligan C, Tessarollo L, Yoshimura T. Monocyte chemoattractant
493 protein-1 (MCP-1), not MCP-3, is the primary chemokine required for monocyte

494 recruitment in mouse peritonitis induced with thioglycollate or zymosan A. J Immunol.
495 2009;183: 3463–3471. doi:10.4049/jimmunol.0802812

496 23. Liao M, Zhou J, Wang F, Ali YH, Chan KL, Zou F, et al. An X-linked Myh11-CreERT2
497 mouse line resulting from Y to X chromosome-translocation of the Cre allele. Genesis.
498 2017;55. doi:10.1002/dvg.23054

499 24. Warthi G, Faulkner JL, Doja J, Ghanam AR, Gao P, Yang AC, et al. Generation and
500 comparative analysis of an Itga8-CreERT2 mouse with preferential activity in vascular
501 smooth muscle cells. Nat Cardiovasc Res. 2022;1: 1084–1100. doi:10.1038/s44161-
502 022-00162-1

503 25. Bjørklund MM, Hollensen AK, Hagensen MK, Dagnæs-Hansen F, Christoffersen C,
504 Mikkelsen JG, et al. Induction of Atherosclerosis in Mice and Hamsters Without
505 Germline Genetic Engineering. Circ Res. 2014;114: 1684–1689.
506 doi:10.1161/CIRCRESAHA.114.302937

507 26. Schindelin J, Arganda-Carreras I, Frise E, Kaynig V, Longair M, Pietzsch T, et al. Fiji:
508 an open-source platform for biological-image analysis. Nat Methods. 2012;9: 676–
509 682. doi:10.1038/nmeth.2019

510 27. Miyoshi T, Tian J, Matsumoto AH, Shi W. Differential response of vascular smooth
511 muscle cells to oxidized LDL in mouse strains with different atherosclerosis
512 susceptibility. Atherosclerosis. 2006;189: 99–105.
513 doi:10.1016/j.atherosclerosis.2005.12.001

514 28. Dikkers A, Freak de Boer J, Annema W, Groen AK, Tietge UJF. Scavenger receptor
515 BI and ABCG5/G8 differentially impact biliary sterol secretion and reverse cholesterol
516 transport in mice. Hepatology. 2013;58: 293–303. doi:10.1002/hep.26316

517 29. Martos-Rodríguez CJ, Albarrán-Juárez J, Morales-Cano D, Caballero A, MacGrogan
518 D, de la Pompa JL, et al. Fibrous Caps in Atherosclerosis Form by Notch-Dependent
519 Mechanisms Common to Arterial Media Development. Arterioscler Thromb Vasc Biol.
520 2021;41: e427–e439. doi:10.1161/ATVBAHA.120.315627

521 30. Basatemur GL, Jørgensen HF, Clarke MCH, Bennett MR, Mallat Z. Vascular smooth
522 muscle cells in atherosclerosis. Nat Rev Cardiol. 2019;16: 727–744.
523 doi:10.1038/s41569-019-0227-9

524 31. Bentzon JF, Otsuka F, Virmani R, Falk E. Mechanisms of plaque formation and
525 rupture. Circ Res. 2014;114: 1852–1866. doi:10.1161/CIRCRESAHA.114.302721

526 32. Wirka RC, Wagh D, Paik DT, Pjanic M, Nguyen T, Miller CL, et al. Atheroprotective
527 roles of smooth muscle cell phenotypic modulation and the TCF21 disease gene as
528 revealed by single-cell analysis. Nat Med. 2019;25: 1280–1289. doi:10.1038/s41591-
529 019-0512-5

530 33. Kim JB, Zhao Q, Nguyen T, Pjanic M, Cheng P, Wirka R, et al. Environment-Sensing
531 Aryl Hydrocarbon Receptor Inhibits the Chondrogenic Fate of Modulated Smooth

532 Muscle Cells in Atherosclerotic Lesions. Circulation. 2020;142: 575–590.
533 doi:10.1161/CIRCULATIONAHA.120.045981

534 34. Shankman LS, Gomez D, Cherepanova OA, Salmon M, Alencar GF, Haskins RM, et
535 al. KLF4-dependent phenotypic modulation of smooth muscle cells has a key role in
536 atherosclerotic plaque pathogenesis. Nat Med. 2015;21: 628–637.
537 doi:10.1038/nm.3866

538 35. Jacobsen K, Lund MB, Shim J, Gunnersen S, Füchtbauer E-M, Kjolby M, et al.
539 Diverse cellular architecture of atherosclerotic plaque derives from clonal expansion
540 of a few medial SMCs. JCI Insight. 2017;2: e95890. doi:10.1172/jci.insight.95890

541 36. Chappell J, Harman JL, Narasimhan VM, Yu H, Foote K, Simons BD, et al. Extensive
542 Proliferation of a Subset of Differentiated, yet Plastic, Medial Vascular Smooth Muscle
543 Cells Contributes to Neointimal Formation in Mouse Injury and Atherosclerosis
544 Models. Circ Res. 2016;119: 1313–1323. doi:10.1161/CIRCRESAHA.116.309799

545 37. Alencar GF, Owsiany KM, Karnewar S, Sukhavasi K, Mocci G, Nguyen AT, et al.
546 Stem Cell Pluripotency Genes Klf4 and Oct4 Regulate Complex SMC Phenotypic
547 Changes Critical in Late-Stage Atherosclerotic Lesion Pathogenesis. Circulation.
548 2020;142: 2045–2059. doi:10.1161/CIRCULATIONAHA.120.046672

549 38. Wang Y, Gao H, Wang F, Ye Z, Mokry M, Turner AW, et al. Dynamic changes in
550 chromatin accessibility are associated with the atherogenic transitioning of vascular
551 smooth muscle cells. Cardiovasc Res. 2022;118: 2792–2804.
552 doi:10.1093/cvr/cvab347

553 39. Lusis AJ, Yu J, Wang SS. The problem of passenger genes in transgenic mice.
554 Arterioscler Thromb Vasc Biol. 2007;27: 2100–2103.
555 doi:10.1161/ATVBAHA.107.147918

556 40. Shi C, Jia T, Mendez-Ferrer S, Hohl TM, Serbina NV, Lipuma L, et al. Bone marrow
557 mesenchymal stem and progenitor cells induce monocyte emigration in response to
558 circulating toll-like receptor ligands. Immunity. 2011;34: 590–601.
559 doi:10.1016/j.immuni.2011.02.016

560

561

562

563

564

565

566

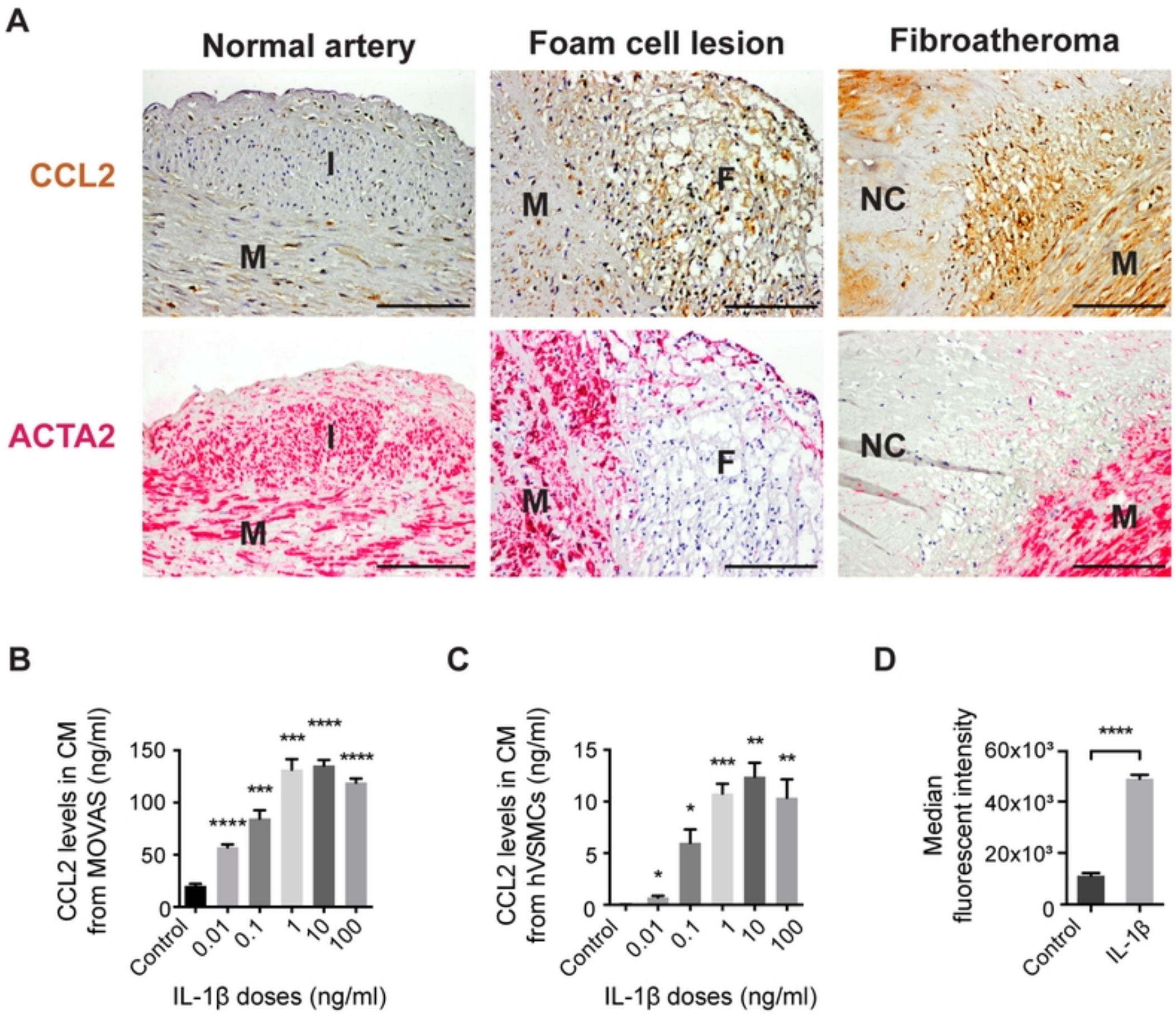
A
Normal artery
Foam cell lesion
Fibroatheroma
CCL2
ACTA2
I
M
F
NC
B
C
D
CCL2 levels in CM from MOVAS (ng/ml)
CCL2 levels in CM from hVSMCs (ng/ml)
IL-1β doses (ng/ml)
Control
0.01
0.1
1
10
100
Median fluorescent intensity
60x10³
40x10³
20x10³
IL-1β

Fig 1

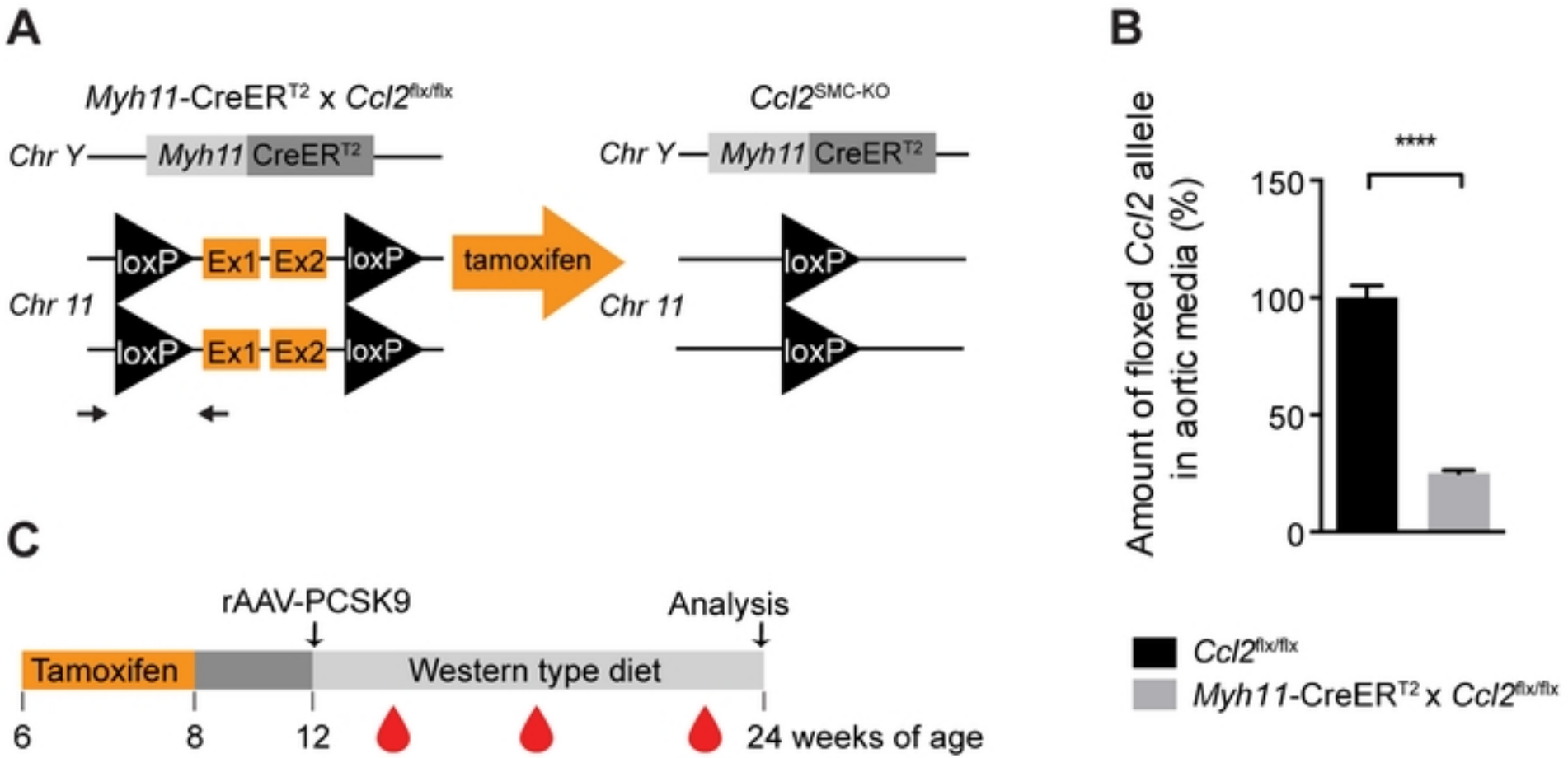
A
Myh11-CreERT2 x Ccl2flx/flx
Chr Y
Myh11 CreERT2
Chr 11
loxP
Ex1
Ex2
loxP
tamoxifen
Ccl2SMC-KO
Chr Y
Myh11 CreERT2
Chr 11
loxP
B
Amount of floxed Ccl2 allele in aortic media (%)
****
150
100
50
0
Ccl2flx/flx
Myh11-CreERT2 x Ccl2flx/flx
C
rAAV-PCSK9
Analysis
Tamoxifen
Western type diet
6
8
12
24 weeks of age

Fig 2

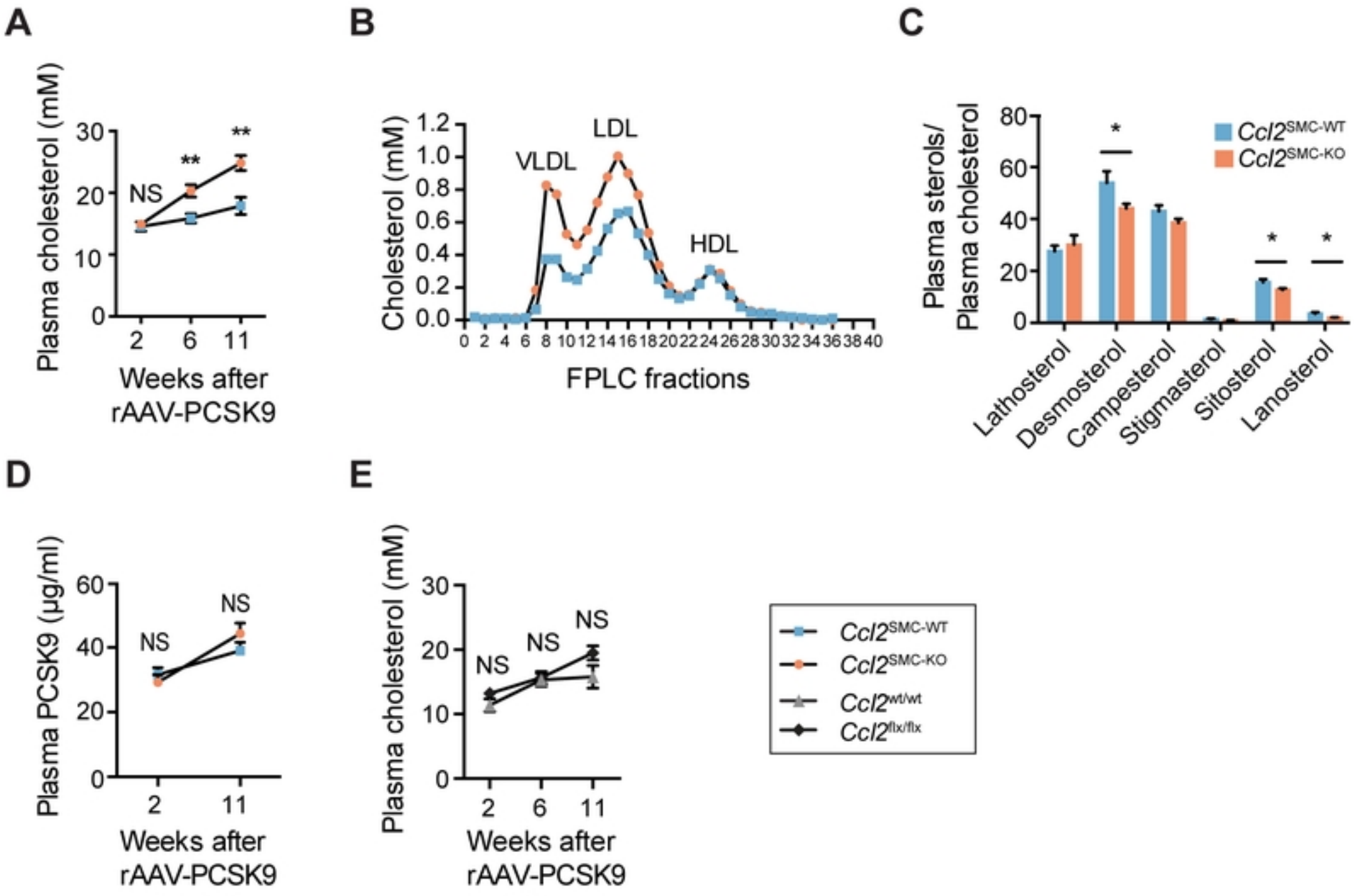
A
Plasma cholesterol (mM)
30
20
10
0
NS
**
**
2
6
11
Weeks after
rAAV-PCSK9
B
Cholesterol (mM)
1.2
1.0
0.8
0.6
0.4
0.2
0.0
VLDL
LDL
HDL
0 2 4 6 8 10 12 14 16 18 20 22 24 26 28 30 32 34 36 38 40
FPLC fractions
C
Plasma sterols/
Plasma cholesterol
80
60
40
20
0
*
*
*
Ccl2SMC-WT
Ccl2SMC-KO
Lathosterol
Desmosterol
Campesterol
Stigmasterol
Sitosterol
Lanosterol
D
Plasma PCSK9 (μg/ml)
60
40
20
0
NS
NS
2
11
Weeks after
rAAV-PCSK9
E
Plasma cholesterol (mM)
30
20
10
0
NS
NS
NS
2
6
11
Weeks after
rAAV-PCSK9
Ccl2SMC-WT
Ccl2SMC-KO
Ccl2wt/wt
Ccl2flx/flx

Fig 3

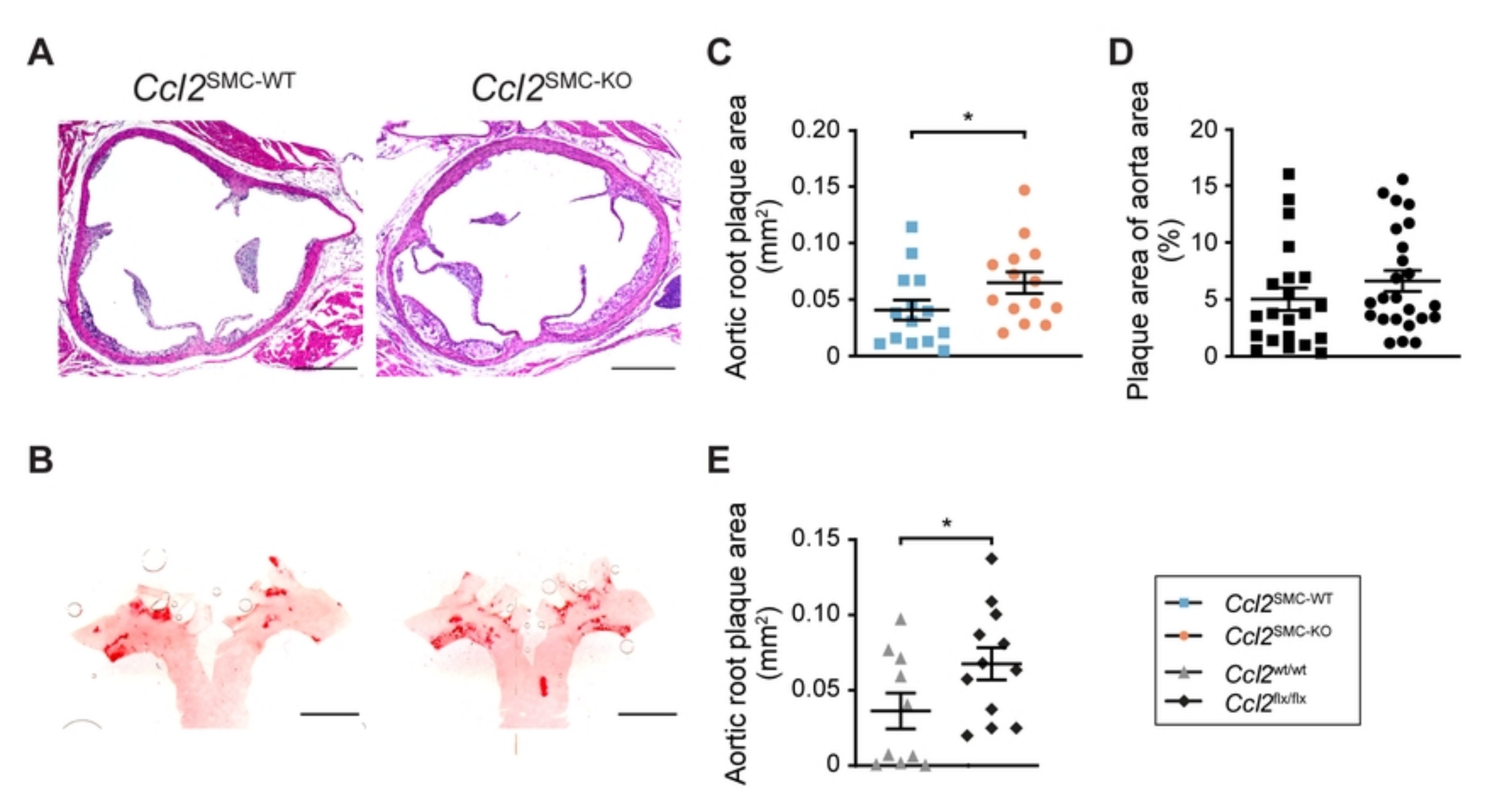
A
Ccl2SMC-WT
Ccl2SMC-KO
B
C
Aortic root plaque area (mm2)
0.20
0.15
0.10
0.05
0
*
D
Plaque area of aorta area (%)
20
15
10
5
0
E
Aortic root plaque area (mm2)
0.15
0.10
0.05
0
*
Ccl2SMC-WT
Ccl2SMC-KO
Ccl2wt/wt
Ccl2flx/flx

Fig 4

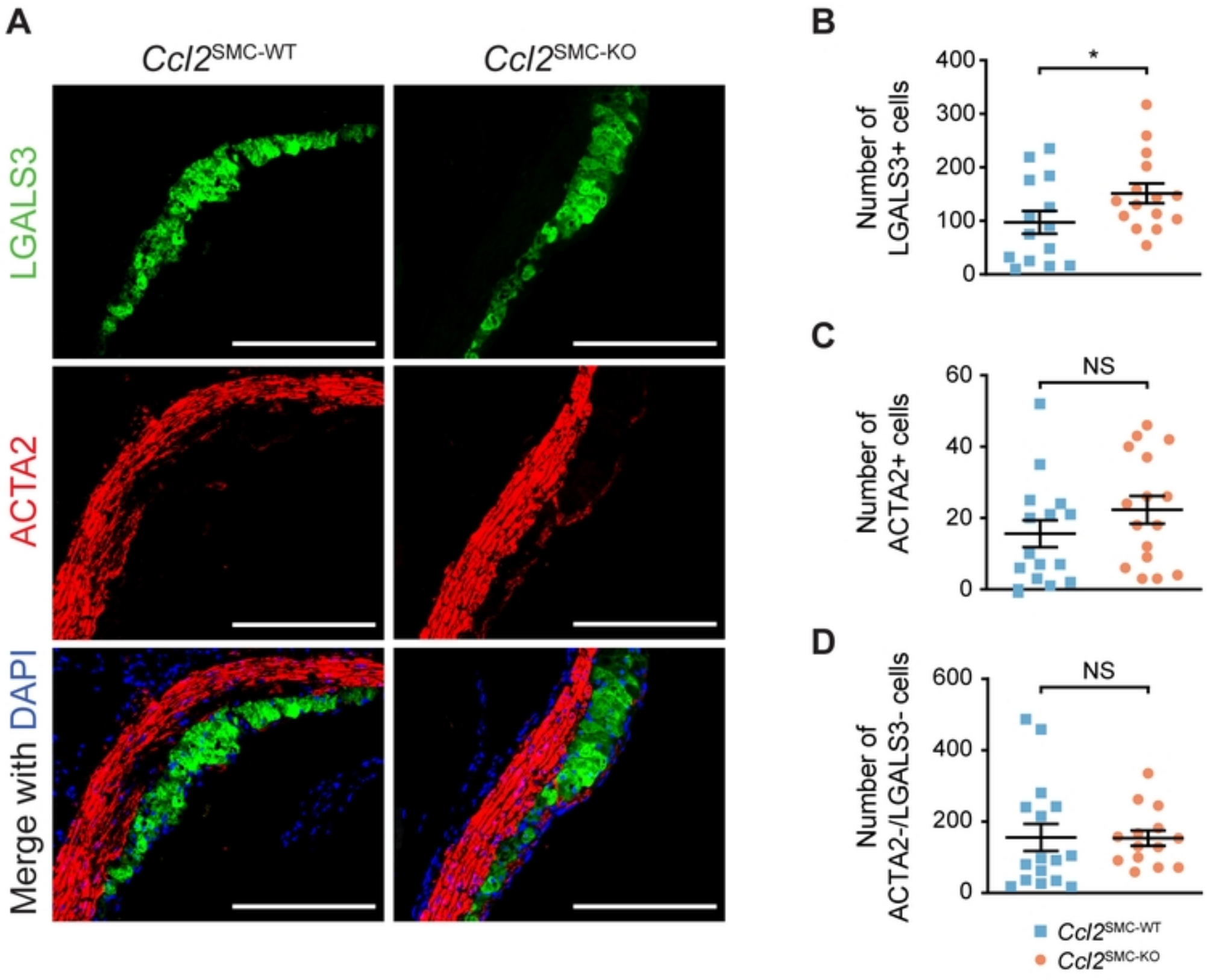
A
Ccl2SMC-WT
Ccl2SMC-KO
LGALS3
ACTA2
Merge with DAPI
B
Number of LGALS3+ cells
400
300
200
100
0
*
C
Number of ACTA2+ cells
60
40
20
0
NS
D
Number of ACTA2-/LGALS3- cells
600
400
200
0
NS
Ccl2SMC-WT
Ccl2SMC-KO

Fig 5